

12. M. N. Kogan, The Dynamics of Rarefied Gases [in Russian], Nauka, Moscow (1967).
13. V. G. Trusov, S. A. Bardak, V. P. Turov, et al., "An automated system of thermodynamic data and calculations of equilibrium states," in: Mathematical Methods of Chemical Thermodynamics [in Russian], Nauka, Novosibirsk (1982).
14. S. Taneda, "Studies of wake vortices, experimental investigation of wake behind a sphere at low Reynolds numbers," J. Phys. Soc. Jpn., 11, No. 10 (1956).
15. Y. S. Lee, Y. P. Chyon, and E. Pfender, "Particle dynamics and particle heat and mass transfer in thermal plasmas. Pt. II. Particle heat and mass transfer in thermal plasmas," Plasma Chem. Plasma Proc., 5, No. 4 (1985).
16. L. D. Landau and E. M. Lifshits, Hydrodynamics [in Russian], Nauka, Moscow (1986).
17. A. W. Baily and J. Hiatt, "Sphere drag coefficients for a broad range of Mach and Reynolds numbers," AIAA J., 10, No. 11 (1972).

DEVELOPING MODELS TO CALCULATE THE EXCHANGE OF HEAT
UNDER CONDITIONS OF SUPERSONIC TURBULENT DETACHED FLOWS

A. A. Zheltovodov, E. G. Zaulichnyi, and V. M. Trofimov

UDC 536.24:532.54

Research into the processes of heat exchange in various turbulent flows is of great theoretical and practical interest. Among the more complex and urgent problems of aerogas-dynamics we can include, with considerable certainty, the study of turbulent detached flows [1]. At supersonic flow velocities the determination of heat-exchange intensity in the vicinity of the separation zones assumes particular importance [2]. With significant changes in the level of turbulence within the external flow, in the boundary layers at the walls, and in the detached intermixing layers [3], methods based on simple correlations of heat-exchange parameters with characteristic pressures, see, for example [4-6], are rather limited. The approach proposed in [7] that is based on the utilization of a model of a nonequilibrium boundary layer seems to be more promising, and in addition to the factors of compressibility, nonisothermicity, and others, which are dealt with in this method in addition to the factors considered within the framework of asymptotic theory [8], the influence of a change in the intensity of large-scale turbulence is also considered. The heat-exchange calculations conducted in [7] for the vicinity of a cavity are in good agreement with the experimental data and the development of such an approach can expediently be applied to other conditions. It is with this purpose in mind that we have conducted additional experimental studies into the quasi-two-dimensional separation of flow in the vicinity of inclined protrusions and recesses [9]. The chosen geometric configuration has enabled us to analyze the effect of sequential interaction between the turbulent boundary layer and the compression shock and rarefaction waves insofar as these related to the intensity of heat exchange. Resort to the extensive additional information derived for these situations in [3, 10, 11] on the basis of utilizing a complex of various diagnostic methods: visualization of the extreme streamlines, optical and pneumometric measurements of pressure and velocity fields, thermoanemometric measurements of the characteristics of turbulence, all of these have enabled us to refine flow structure and the characteristic physical properties in order to validate the computational model being developed here with respect to new conditions.

Heat-exchange measurements were conducted in a wind tunnel with an operating wind-stream diameter of 304 mm within an Eifel chamber at incident-flow Mach numbers of $M_1 = 2, 3,$ and 4. The individual Reynolds numbers varied within a range of $Re_1 = (30-91) \cdot 10^6 \text{ m}^{-1}$, the deceleration pressure $p^* = 200-1540 \text{ kPa}$, and the deceleration temperature $T^* = 255-270 \text{ K}$.

The studied configurations formed an inclined step oriented counter to the flow (Fig. 1b) or an inclined recess, streamlined in the opposite direction, with a fixed height $h = 6 \text{ mm}$ and a face deflection angle of $\beta = 25^\circ$. The distance from the leading edge of the plate to the apex of the compression angle in the case of the protruding step amounted to 141 mm, and to 150 mm in the case of the apex of the expansion angle on the model of the re-

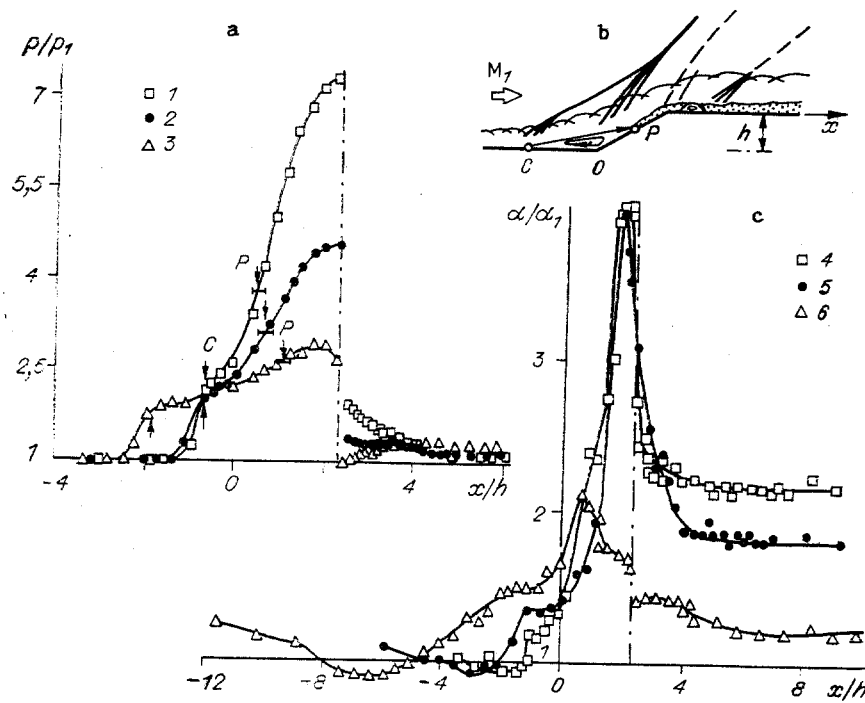


Fig. 1

cess. The ratio of the width of the model to the height of the barrier is given by $b/h = 20$. A 4-mm wide strip designed to create turbulence was attached with glue at a distance of 6 mm from the leading edge of the plate, with a stand-roughness height of 0.2 mm. The thickness of the unperturbed boundary layer in front of the interaction zones involving the shock or rarefaction waves came to $\delta = 2.5-2.6$ mm. For purposes of electrical installation and to reduce the removal of heat to the wall by means of heat conduction, the central portion of the model, at which thermocouples were used to measure the intensity of the heat exchange, is made out of textolite. The model design is described in greater detail in [9]. A modification of the electrocalorimetric method [12] is used to measure heat exchange, and according to this method the heating element consists of a current-conducting film based on graphite. The total measurement error for the coefficient α of heat-exchange intensity is guaranteed, in this case, not to exceed 15%.

The research conducted into the exchange of heat that occurs in the streamlining of an inclined protruding step was confirmed and enhanced with the quantitative relationships observed in [3, 11] insofar as these pertain to the development of flow separation under these conditions. Following these studies, the reduction in M_1 for fixed β and h , as well as the increase in β for constant M_1 and h , leads to the appearance and growth of a separation zone in the vicinity of the compression angle, as well as to the formation, at a certain stage, of a region of a positive pressure gradient, which is followed by a local detachment of the flow beyond the apex of the expansion angle (see Fig. 1b). The data derived in the studies with respect to pressure distribution when $\beta = 25^\circ$, $h = 15$ mm, $h/\delta = 3.3-3.9$ (Fig. 1a) characterize the cited unique features in the development of the flow (1-3: $M_1 = 4, 3$, and 2.2). The arrows indicate the positions of the runoff (separation) lines C and the runoff (connecting) lines P, while the vertical dashed-dotted line shows the position of the expansion apex; p_1 represents the pressure at the surface of the plate in an unperturbed flow.

The distribution of the local coefficient of heat-exchange intensity α , referred to the characteristic value of α_1 in front of the interaction region (Fig. 1c) qualitatively reflects the main features of the flow, which follow out of the pressure distribution (4: $M_1 = 4$, $Re_1 = 41 \cdot 10^6 \text{ m}^{-1}$; 5 and 6: $M_1 = 3$ and 2 , $Re_1 = 31 \cdot 10^6 \text{ m}^{-1}$). In particular, with a drop in M_1 we observe an increase in the extent of the separation in front of the compression angle and a reduction in the heat-exchange level in the zone in which the lines connect on the inclined face. During the course of the expansion taking place behind the apex, and this passes through the rarefaction wave, we have a gradual reduction in heat-exchange intensity and when $M_1 = 2$ (conventional notation 6) the nature of the distribution in the

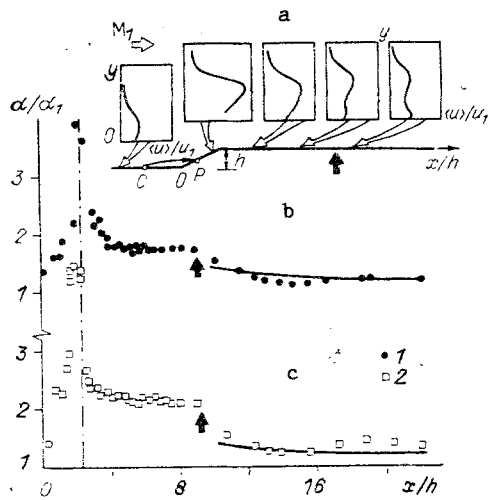


Fig. 2

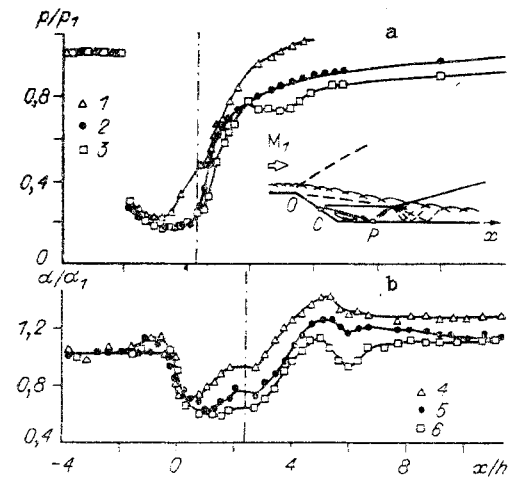


Fig. 3

quantity α/α_1 reflects the existence of repeated local separation, analogous to pressure distribution. The insignificant difference between the maxima in heat exchange at the compression surface for the case in which $M_1 = 3$ and 4, in comparison to the pressure changes observed in Fig. 1a, can be ascribed to the lower relative height of the barrier ($h/\delta = 2.3-2.4$) in the former case, as a consequence of which the relative extent of the flow on the inclined surface will also be somewhat smaller and will limit the anticipated changes in heat exchange.

A remarkable feature is the reverse trend in the behavior of the exchange of heat in front of the barrier as the Mach number changes (Fig. 1c, $x/h < 0$) in comparison to the pressure distribution (Fig. 1a). Thus, the pressure in the region of the forming plateau (an isobaric zone) between the runoff and dispersal flow lines increases as M_1 increases. At the same time, in the distribution of the heat-exchange factors, under analogous conditions, we observe a drop in its "plateau" values. It might be assumed that the explanation for this effect is the possibility, observed in [3, 13, 14] on the basis of an analysis of velocity profiles, for a change in the state in the return flow in the separation zones, as well as in the case of the relaminarization of the flow near the wall. According to the cited studies, such conditions arise as a consequence of the effect of the negative pressure gradient in the direction of the reverse flow, as well as a result of the reduction in the local Reynolds number, ascribed to the drop in velocity on approach to the point of separation.

A significant difference in the change of the heat-exchange level in comparison to pressure, in dependence on M_1 , has been observed at the upper surface of the barrier, beyond the rarefaction waves (see Fig. 1c, $x/h > 4$). Despite the fact that the pressure in this region, for various Mach numbers, remains virtually identical and close to the characteristic value for the unperturbed flow (Fig. 1a), the level of heat exchange increases intensively as M_1 rises. Such behavior is quite correct, considering the elevated level of turbulent pulsations recorded in [3] in the dissipative flow at the upper surface of the protruding step, as well as the indications of the formation of a new thin boundary layer in the region near the wall [3, 11, 13], shown in Fig. 1b. Here, the Toepler photographs obtained with the aid of a pulsed light source [11] made it possible to establish large-scale coherent vortex structures in the outer region of the dissipative flow, these structures developing in the mixing layer above the separation zone in the compression angle. In accordance with the measurements taken in [3], it is precisely in this region that there arises the characteristic maximum in velocity pulsations as a result of the interaction of the boundary layer with the compression shock in the vicinity of the points of separation and connection, maintained for some extent in the flow at the upper surface of the protruding step (Fig. 2a). It is noteworthy that the clearly observed reduction in heat-exchange intensity at a distance of $x/h \approx 9-13$ (Fig. 2b, c: 1: $M_1 = 3$; 2: $M_1 = 4$) is observed on attainment of the region (Fig. 2a, the black arrow) where generation of turbulence begins to predominate in the portion of the flow at the wall, and where the pulsation maximum increasing at the surface exceeds the level that is characteristic for the outer regions. According to [3, 11, 13], the profiles of the average velocities in this region are close

to those that are typical for an unperturbed boundary layer. When we take into consideration the thickness of the boundary layer at the upper surface of the barrier, namely $\delta \approx h$, the extent of the zone is virtually constant and the elevated intensity of heat exchange beyond the flare of the rarefaction waves $\Delta x/h = 5.3-6.3$ corresponds to the estimate from [3] for the relaxation length of the large-scale turbulence, amounting approximately to $(5-6)\delta$.

The data derived in [10] with respect to the structure of the flow and the distribution of pressure in the vicinity of the inclined recessed step, with a face angle of deviation $\beta = 25^\circ$, and a height $h = 15$ mm ($h/\delta \approx 2.8$) (Fig. 3a, 1-3: $M_1 = 2.2, 3,$ and 4 , respectively, $Re_1 = 25 \cdot 10^6, 32 \cdot 10^6,$ and $58 \cdot 10^6$ m⁻¹) allows us to explain certain of the features observed in the exchange of heat. It is obvious that they are, to a considerable extent, determined by the sequence of boundary-layer interactions with the rarefaction waves and compression shocks that are reversed relative to the protruding step (Fig. 3b, 4-6: $M_1 = 2.2, 3,$ and 4 ; $Re_1 = 40 \cdot 10^6, 31 \cdot 10^6,$ and $56 \cdot 10^6$ m⁻¹, respectively). There is a noticeable drop in the intensity of heat exchange beyond the apex of the expansion angle. In front of the separation zone, in the vicinity of the apex of the compression angle, identified by the dashed-dotted line in the figures, there is a growth in α/α_1 and we observe stratification in the experimental data with respect to M_1 . The lower values of M_1 correspond to a higher level of heat exchange. In the separation zones we observe a trend toward the formation of a plateau region. After the flow links together beyond the compression angle the higher level of heat exchange also corresponds to lower M_1 numbers. The quantity α/α_1 continues to increase for some distance beyond the connecting point to a maximum value, and this is then followed by a noticeable drop, with formation of a minimum. An analogous minimum is also observed in the distribution of pressure at $M_1 = 4$ (Fig. 3a, 3). According to [10], it can be ascribed to the influence exerted by the rarefaction waves emanating out of the triple point of the λ configuration of the compression shock in the vicinity of the separation zone, as shown in the diagram and directed toward the surface. For the case in which $M_1 = 2.2$ (conventional notation 1) no such minimum is observed, but we observe only a reduction in the rate of pressure rise. At the same time, the change in the intensity of the heat exchange in this region remains quite noticeable. It might be assumed that with a reduction in M_1 owing to removal of the triple point from the surface, and owing also to the reduction in the intensity of the rarefaction waves emanating from that surface, their influence on the flow near the wall becomes less localized. With rising M_1 the influence of the waves intensifies and promotes reduction of heat exchange downstream. A significant contribution to the process under these conditions is made also by the rise in the intensity of the rarefaction wave flare, suppressing turbulence, in front of the compression angle. According to the data derived in [9], the effect of such waves in the case of fixed M_1 increases as Re declines, reducing the intensity of the heat exchange beyond the barrier.

The increase in α/α_1 in the distant flow beyond the inclined recess, with a reduction in M_1 (see Fig. 3b) to a considerable extent is also associated with the observed increase in the extent of the separation zone in front of the apex of the compression angle and correspondingly to the additional increase in turbulent pulsations in the outer region of the mixing layer.

The measurements which have been carried out demonstrated that the maximum increment in the relative intensity of the exchange of heat beyond the inclined recess, in comparison to the characteristic value for the flow in front of that recess, under the conditions being examined here did not exceed 10-35%. At the same time, behind the inclined protruding step the analogous quantity increased by a factor of 1.5-2. Thus, the sequence in which the rarefaction waves and the compression shock interact with the turbulent boundary layer significantly affect the intensity of the exchange of heat in the perturbed flow.

Newly derived experimental data dealing with the unique features of the separation streamlining of inclined steps and recesses, as well as with the nature of heat exchange in the vicinity of such barriers, provided a basis for verification and subsequent development of the computational model proposed in [7]. In accordance with this model, in calculating the heat-exchange intensity in the vicinity of the separation zones under conditions of compressible turbulent boundary layers, use should be made of the concept of a new boundary layer in the region behind the connecting point, whose development might be analyzed within the framework of asymptotic theory [8]. Of fundamental importance here is the need to account for an additional factor which characterizes the influence of the external large-scale turbulence at the new layer, together with the earlier-employed factors

of compressibility, nonisothermicity, etc. Consideration of external turbulence can be accomplished, for example, on the basis of the relationship proposed in [15] for incompressible flows, where the level of turbulence under these conditions must be determined from the experimentally found maximum level of velocity pulsations for the outer region of boundary layers perturbed by separation. The validity of accounting only for pulsations in velocity under the conditions of compressible flows follows out of asymptotic theory [8], according to which in the relationship for the density of the heat flow along the normal to the surface within the core of the turbulent boundary layer $q = -c_p \rho \langle uT \rangle (1 - \beta_T)$ the quantity $\beta_T \sim (u \langle \nu u T \rangle) / \langle \nu u \rangle T$, accounting for the effect of pulsations in density on the turbulent transfer of heat, tends to zero as $Re \rightarrow \infty$. The validity of such concepts for finite Re is also rather well founded in [8]. When we take into consideration the measurement results obtained in [3] for the characteristics of turbulence in the separated mixing layers and in the connecting boundary layers, according to which the pulsations in density near the walls are smaller by virtually one order of magnitude than the pulsations in velocity, we note that in such situations it is, apparently, correct to neglect the influence of density pulsations on the intensity of the exchange of heat at the surface.

In calculating heat exchange, as in [7], we will use the integral energy equation for a two-dimensional boundary layer, which for a nonpermeable surface in the absence of internal sources of heat release, can be represented in the form

$$\frac{d Re_T^{**}}{dx} + \frac{Re_T^{**}}{\Delta T} \frac{d\Delta T}{dx} = Re_L St_0 \Pi \psi_i, \quad (1)$$

where Re_T^{**} is the Reynolds number, constructed on the basis of the energy loss thickness; $\Delta T = T_w - T_w^*$, $x = x/L$ (L is a characteristic dimension); $Re_L = \rho_e u_e L / \mu^*$ (μ^* is the coefficient of dynamic viscosity at the deceleration temperature T^*); $\Pi \psi_i$ is the product of the perturbing factors. Following the methods of asymptotic theory for a turbulent boundary layer [8], we will introduce the law governing heat exchange under standard conditions and in the absence of perturbation factors:

$$St_0 = \frac{0.0128}{(Re_T^{**})^{0.25} Pr^{0.75}} \left(\frac{\mu_w}{\mu_w^*} \right)^{0.25} \quad (2)$$

as well as the limit relative heat-exchange (friction) law, taking into consideration the effect of these factors. Thus, in the presence of compressibility and nonisothermicity, according to [8], the expression for the limit relative law is represented by the product

$$\psi = \psi_M \psi_T = \left[\frac{\text{arctg } M_e \sqrt{r \frac{k-1}{2}}}{M_e \sqrt{r \frac{k-1}{2}}} \right]^2 \left[\frac{2}{\sqrt{T_w/T_w^* + 1}} \right]^2$$

(M_e is the Mach number at the outer edge of the boundary layer and r is the recovery factor).

As demonstrated in [16], the influence of certain additional perturbation factors can be written as $\psi = \Pi \psi_i$. Comparison of such a representation with numerical calculations showed good agreement. Making use of this, in analogous fashion we will introduce a factor for large-scale turbulence ψ_ε applicable to nonequilibrium boundary layers and we will derive an expression $\psi = \psi_M \psi_T \psi_\varepsilon$ for the relative law. Owing to the absence of a noticeable change ΔT along the surface, Eq. (1) in conjunction with (2) is simplified as follows:

$$\frac{d(Re_T^{**})^{1.25}}{dx} = Re_L \frac{0.0128}{Pr^{0.75}} \left(\frac{\mu_w}{\mu_w^*} \right)^{0.25} \Pi \psi_i.$$

Integration yields

$$Re_T^{**} = \left[0.0128 \frac{Re_L^*}{Pr^{0.75}} \int_0^{\bar{x}} \Pi \psi_i \left(\frac{\mu_w}{\mu_w^*} \right)^{0.25} \frac{\rho_e u_e}{\rho^* u_{\max}} d\bar{x} \right]^{0.8}$$

$$\left(Re_L^* = \frac{\rho^* u_{\max} L}{\mu^*}, u_{\max} = \sqrt{2c_p T^*} \right).$$

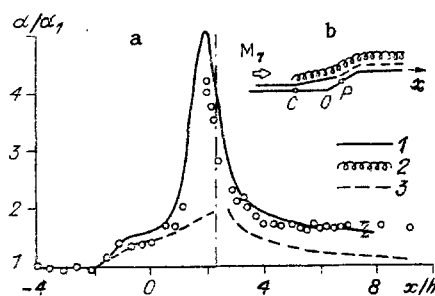


Fig. 4

The local Stanton numbers $St = St_0 \Pi \psi_i$ and the coefficient of heat-exchange intensity $\alpha = c_p \rho u St$.

With regard to the separation flows under consideration here, the factor ψ_e , in analogy with the relationship proposed in [15] to account for changes in the turbulence of the external flow, includes the instantaneous intensity of the maximum of velocity pulsations $\langle u \rangle_m$ in the outer region of the boundary layer on passage of a compression shock or rarefaction waves, as well as the initial level of $\langle u_1 \rangle$ characteristic for the incoming flow outside of the boundary layer:

$$\psi_e = 1 + \frac{200}{u_1^2} (\langle u \rangle_m - \langle u_1 \rangle)^2. \quad (3)$$

The generalization validated in [9] that is based on an analysis of the simplified equation proposed in [17] for the kinetic energy of turbulence enabled us to establish a flow determined primarily by three-dimensional deformations, as well as the experimentally confirmed interrelationship between $\langle u \rangle_m$ and the instantaneous pressure p at the surface in the zone of free interaction in the vicinity of the separation points:

$$\frac{\langle u \rangle_m - \langle u_1 \rangle_m}{\langle u_p \rangle_m - \langle u_1 \rangle_m} = \frac{p - p_1}{p_p - p_1} = F(x/\delta) \quad (4)$$

(the subscript p pertains to parameters in the region of the pressure plateau, δ is the thickness of the boundary layer immediately ahead of the point at which the rise in pressure sets in, and x is the longitudinal coordinate reckoned from this point). According to [9], data from various authors are satisfactorily approximated by the function

$$F(x/\delta) = 1 - \exp[-0.077(x/\delta)^2]. \quad (5)$$

It is essential that relationships (4) and (5) remain equally valid for the connection zones and that they can be utilized to carry out calculations on transition through the dispersion line. In this case, the pressures behind the point of connection, characteristic for the maximum pressure zone, correspond to the parameters in (4) for the plateau region, while those parameters identified with the subscript 1 correspond to the characteristics in the plateau region, including the local thickness δ of the boundary layer, in analogy with the separation points.

The results from the calculation of the heat-exchange characteristics in the vicinity of the inclined protruding step for the case in which $M_1 = 3$, $Re_1 = 31 \cdot 10^6 \text{ m}^{-1}$, derived through resort to the data from [11] on the distribution of pressure, are shown by a solid line in Fig. 4a. In accordance with the simplified physical model of such a flow (Fig. 4b), the thermal boundary layer (conventionally identified 1) was calculated from its physical origin within the framework of asymptotic theory, with consideration given to the factors of compressibility and nonisothermicity. Beginning from the point of the onset of pressure increase in front of the compression angle, we took into consideration the factor ψ_e (conventional sign 2), which was found on the basis of Eq. (3) and generalizations (4) and (5). Between the separation and connection points the flow was found to be the same as over a solid surface along a separating streamline. In this connection, the results here are conditional, although quite near to those of the experiment (see Fig. 4a). In the case of large-scale separation [7] it would be more correct to carry out the calculation with consideration of the parameters of reverse flow and the levels of turbulence within the mixing layer. At the same time it is obvious that under the conditions of limited (about 7δ) extent of

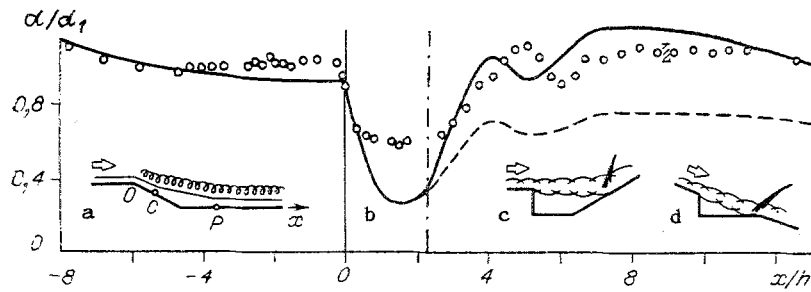


Fig. 5

the separation zone the utilization of a more simplified model is quite acceptable from a practical standpoint. From the connection point, as well as from the effective starting point, a new layer is calculated (see Fig. 4b, conventional sign 3), for which the external region of the old layer performs the function of the external flow. The quantity ψ_ϵ behind the rarefaction waves is determined on the basis of turbulence measurements [3]. As demonstrated in [7], the gradual lowering of pulsation intensity at constant downstream pressure to $x/h = 7$ (Fig. 4b) can also be described in approximate terms by the following relationship which is taken from the theory of thermal streams:

$$\left(\frac{\langle u \rangle - \langle u \rangle_e}{\langle u \rangle_0 - \langle u \rangle_e} \right)^2 = \left(1 + 15.5 \frac{x - x_0}{x_0} \right)^{-0.8},$$

where $\langle u \rangle_0$ represents the maximum of pulsations immediately in front of the apex of the expansion angle, whose coordinate is x_0 ; $\langle u \rangle_e$ is the level of pulsations above the boundary layer, far downstream.

We can see from Fig. 4a that the results of the calculation based on the model examined here are in good agreement with experiment. The vertical dashed band characterizes the accuracy of the thermal measurements. It is significant that analogous calculation without consideration of ψ_ϵ (the dashed line) leads to marked lowering of the heat-exchange level. The solid lines in Fig. 2b, c show the results of the heat-exchange calculations for the new layer in the distant flow and these have been derived with consideration of the pulsation intensity in the outer region of the same level as in the unperturbed boundary layer. It is clear that such an approximation provides for satisfactory prediction of the heat-exchange intensity in this region.

Achievement of acceptable agreement in the calculation of heat-exchange intensity in the vicinity of the inclined recess with experimental results required changes in the physical model of the flow (Fig. 5a), where the effect of the new flare was eliminated. When carrying out calculations within the scope of this model, we took into consideration ψ_M , ψ_T , and ψ_ϵ , and we also made use of the pressure distribution derived in [10]. The reduction in the maximum of the velocity pulsations in the outer region of the boundary layer on passage of rarefaction waves was determined on the basis of the relationship proposed in [18], namely, $\langle u \rangle_m / \langle u_1 \rangle_m = (\rho / \rho_1)^{1/2}$, where ρ is the corresponding local density. In analogy with the foregoing case, with $\beta = 25^\circ$, $M_1 = 4$, $Re_1 = 56 \cdot 10^6 \text{ m}^{-1}$, calculation of the heat exchange without consideration of the changes in ψ_ϵ (Fig. 5b, the dashed line) differs significantly from the experimental data, while consideration of this factor (the solid line) provides for satisfactory agreement.

In view of the diverse nature of the distribution in the velocity of the boundary layers (as noted in [10]) at the protruding steps and behind the recesses the resulting need to eliminate the effect of the new layer in the latter case is not a random event. As demonstrated in the present study, the profiles of the velocity behind the recess virtually do not differ from the characteristic profiles of equilibrium flows. At the same time, according to [3, 11], the significant deformations both in the profiles of the average velocity and in the fluctuations associated with the new layer are preserved for rather long periods of time at the protruding steps. In addition, we earlier established such a layer visually [13]. Because of the memory effect characteristic of turbulent flows we would note that despite the absence of noticeable deformations in the averaged flow behind the inclined recess, the relaxation of the turbulent characteristics may continue for considerable distances. We can see from the cited calculations that these effects can be taken

into consideration through introduction of the factor ψ_ϵ (see Fig. 5a) in conjunction with the maximum level of velocity pulsation in the outer region of the perturbed boundary layer.

The analysis of the derived and known data on heat exchange in the vicinity of the inclined and straight recesses, such as that carried out in [9], showed that a validated computational model which does not take into consideration this new layer remains valid in all situations where separation is preceded by rather intense rarefaction waves. At the same time, elimination of such waves in the case of separation streamlining of the configurations dealt with in [19] (Fig. 5c) led to a significant increase in the intensity of the large-scale turbulence and to the appearance of the new-layer effect behind the connection point. The absence in the present study of heat-exchange data prevented us from verifying the possibility of using the earlier computational model. However, it is significant that the corresponding calculation, carried out in [7], analogous to (with virtually no rarefaction waves) the streamlining of a triangular cavity in the wall of a supersonic nozzle (Fig. 5d), required consideration of this new-layer effect.

Thus, the studies that have been carried out made it possible to expand our concept of the features involved in the exchange of heat under the conditions of separation streamlining of two-dimensional barriers and to develop computational models for its evaluation in the case of various sequences of interaction between the turbulent boundary layer and the compression shocks and rarefaction waves. It is clear that a more penetrating explanation of the noted differences in the flow behind the protruding steps and recesses will require additional data as to the characteristics of turbulence for the latter situation.

LITERATURE CITED

1. L. V. Golish and G. Yu. Stepanov, Turbulent Separation Flows [in Russian], Nauka, Moscow (1979).
2. V. Ya. Borovoi, Gas Flow and Heat Exchange in Zones of Shock-Wave Interaction with a Boundary Layer [in Russian], Mashinostroenie, Moscow (1983).
3. A. A. Zheltovodov and V. N. Yakovlev, "Stages in the development, the structure, and characteristics of turbulence in compressible separation flows in the vicinity of two-dimensional barriers," Preprint No. 27-86, Akad. Nauk SSSR, Sib. Otd. ITPM, Novosibirsk (1986).
4. F. T. Hung and D. O. Barnett, Shock-Wave Boundary Layer Interference Heating Analysis, New York (1973) (Pap./AIAA, No. 237).
5. M. S. Holden, Shock-Wave Turbulent Boundary Layer Interaction in Hypersonic Flow, New York (1977) (Pap./AIAA, No. 45).
6. N. N. Shkirin, "A computational study of local heat flows on transition through a rarefaction flow," Tr. TsAGI, No. 2274 (1985).
7. E. G. Zaulichyi and V. M. Trofimov, "An investigation into the exchange of heat in the separation regions streamlined by a supersonic flow in a Laval nozzle, Zh. Prikl. Mekh. Tekh. Fiz., No. 1 (1986).
8. S. S. Kutateladze and A. I. Leont'ev, The Turbulent Boundary Layer of a Compressed Gas [in Russian], Nauka, Novosibirsk (1962).
9. A. A. Zheltovodov, E. G. Zaulichyi, V. M. Trofimov, and V. N. Yakovlev, "Studying heat exchange and turbulence in compressed separation flows," Preprint, No. 22-87, Akad. Nauk SSSR, Sib. Otd., ITPM, Novosibirsk (1987).
10. A. A. Zheltovodov, L. Ch.-Yu. Mekler, and E. Kh. Shilein, "Features in the development of flow separation in the compression angles behind rarefaction waves," Preprint No. 10-87, Akad. Nauk SSSR, Sib. Otd., ITPM, Novosibirsk (1987).
11. A. A. Zheltovodov, E. Kh. Shilein, and V. N. Yakovlev, "Development of a turbulent boundary layer under conditions of mixed interaction with compression shocks and rarefaction waves," Preprint No. 28-83, Akad. Nauk SSSR, Sib. Otd., ITPM, Novosibirsk (1983).
12. V. N. Zaikovskii, E. G. Zaulichyi, B. M. Melamed, and Yu. M. Senov, "An experimental study into the local coefficients of heat and mass exchange at the walls of a valve device," Zh. Prikl. Mekh. Tekh. Fiz., No. 2 (1982).
13. A. A. Zheltovodov, "Analysis of the properties of two-dimensional flow separation at supersonic velocities," in: A Study of Near-Wall Flows of a Viscous Gas [in Russian], ITPM SO Akad. Nauk SSSR, Novosibirsk (1979).
14. A. A. Zheltovodov, A. A. Pavlov, E. H. Shilein, and V. N. Yakovlev, "Interconnectionship between the flow separation and the direct and inverse transition at supersonic speed conditions," in: 2nd IUTAM Symp. on Laminar-Turbulent Transition, Novosibirsk, 1984, Springer, Berlin-Heidelberg (1985).

15. M. E. Deitch, Technical Gasdynamics [in Russian], Nauka, Moscow (1974).
16. A. I. Leont'ev and E. G. Zaulichyi, "Determination of the relative coefficients of heat and mass exchange and of the critical separation parameters for a turbulent boundary layer on nonuniform injection under conditions of nonisothermicity," *Inzh.-fiz. Zh.*, 19, No. 4 (1970).
17. K. Hayakaw, A. J. Smits, and S. M. Bogdonov, "Experimental research into the characteristics of turbulence in the nearly connected shearing layer within a compressed gas," *Aérokosm. Tekhnika*, 2, No. 12 (1984).
18. J. P. Dussauge and J. Gaviglio, "Bulk dilatation effects on Reynolds stresses in the rapid expansion of a turbulent boundary layer at supersonic speeds," in: *Proc. 3rd Symp. on Turbulent Shear Flows*, California (1981).
19. G. S. Settles, B. K. Baca, D. R. Williams, and S. M. Bogdonoff, *A Study of Reattachment of a Free Shear Layer in Compressible Turbulent Flow*, New York (1980) (Pap./AIAA, No. 1408).

IMPURITY DISPERSION IN NONUNIFORM FLOWS

A. I. Moshinskii

UDC 532.517.2

The theory of impurity dispersion in tubes owes its origin to the work of Taylor [1], where the equation of diffusion was derived with constant coefficients for the impurity concentration averaged over the cross section, this equation replacing the local diffusion equation with convective terms dependent on the coordinate transverse to the flow. Aris [2] subsequently refined the value of the coefficient of effective diffusion (dispersion), he proposed formulas for the coefficient of dispersion in a tube with an arbitrary lateral cross section, and he refined the areas of applicability for the Taylor theory as one which is asymptotic for sufficiently long times. At the present time, the theory of dispersion is covered in a large number of studies. We can cite a number of these, containing unique approaches to the problem [3-5] and refining the Taylor-Aris model for lower time values, and then [6, 7], developing the theory in various directions.

A significant feature of the above-cited and similar studies on the theory of dispersion is the uniformity of fluid motion and the independence of the velocity component relative to the longitudinal coordinate, thus limiting the applicability of the theory, essentially, to prismatic tubes. Whereas in nature and in technology one frequently encounters nonuniform flows that are, in a certain sense, similar to the flow in tubes, in order to describe the propagation of impurities through these tubes it would be desirable to derive the equations of equivalent diffusion, analogous to the Taylor dispersion equation. The solution of this problem for a number of cases is precisely the aim of this study.

1. Dispersion of Impurities in Elongated Zones, in the Nonuniform Flow of a Fluid.

Elongation of a zone indicates that one of the measurements of the flow region considerably exceeds the two remaining measurements, and it is the propagation of the impurity precisely in that direction that is of interest to us. Flows of this kind are formed in the stagnation regions of various pieces of equipment, in tubes when barriers are present, etc. Here and below, we will conduct our study with a coordinate system that is either nonmoving or moving at some mean velocity, as well as for cases in which there is no mean motion in any of the directions we have selected. We will assume the flow of the fluid to be laminar, and the fluid itself to be incompressible. Under these assumptions, the equation of convective diffusion in dimensionless coordinates has the form

$$\varepsilon^2 \frac{\partial c}{\partial t} + \varepsilon \text{Pe} \left(u \frac{\partial c}{\partial x} + v \frac{\partial c}{\partial y} + w \frac{\partial c}{\partial z} \right) = \frac{\partial^2 c}{\partial x^2} + \frac{\partial^2 c}{\partial y^2} + \varepsilon^2 \frac{\partial^2 c}{\partial z^2}, \quad (1.1)$$